Pines et al., http://www.jcb.org/cgi/content/full/jcb.201112132/DC1



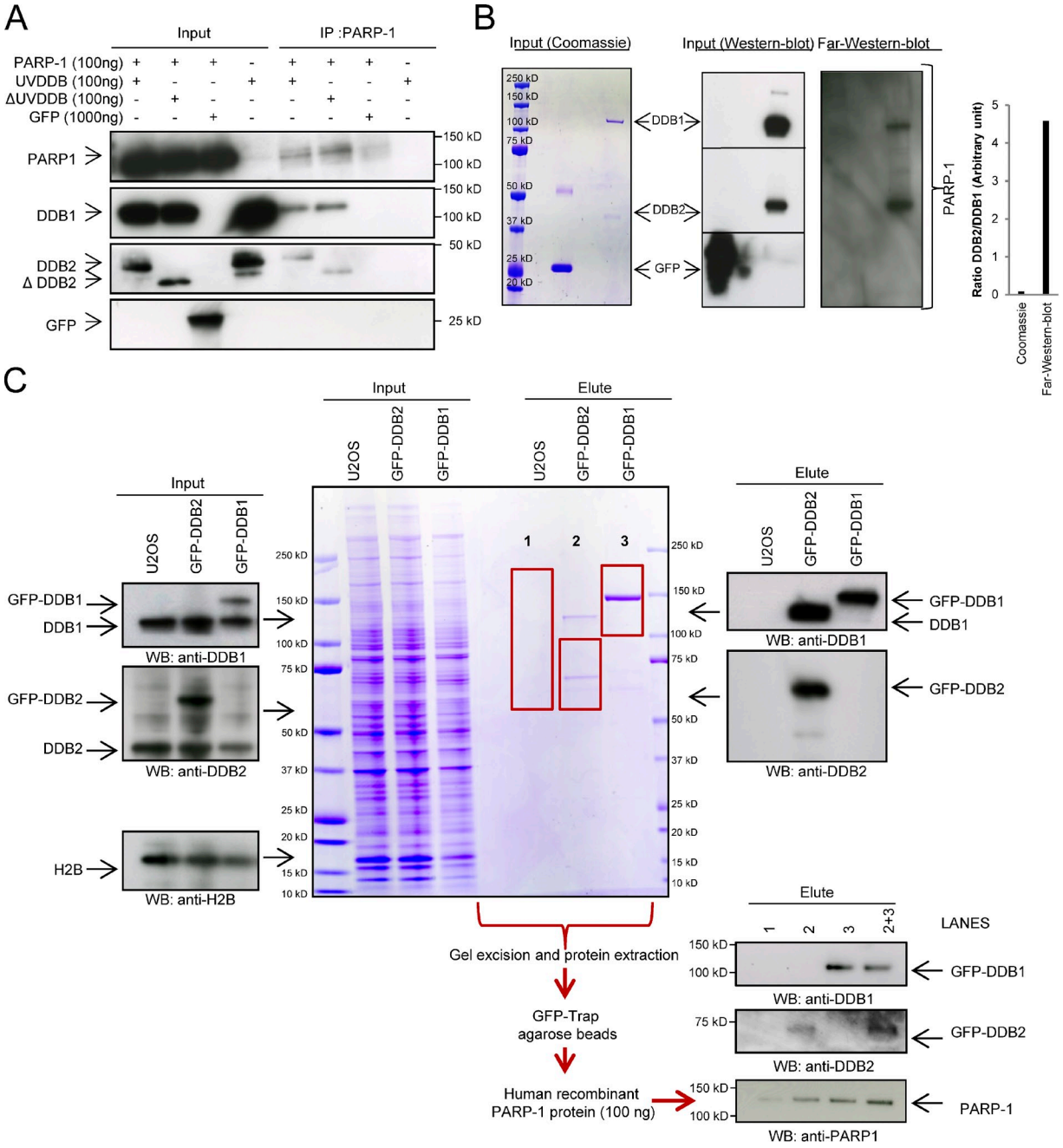


Figure S1. **Direct interaction in vitro between DDB2 and PARP-1.** (A) In vitro coimmunoprecipitation. UV-DDB, ΔUV-DDB (DDB2 lacking its first 40 N-terminal amino acids), and PARP-1 recombinant proteins were used to test direct interaction in vitro. GFP recombinant protein was used as negative control. IP, immunoprecipitate. (B) Far-Western blot assay. UV-DDB recombinant proteins were separated by SDS-PAGE, transferred to a membrane, and incubated with 10 µg/ml PARP-1 recombinant protein. The PARP-1 binding was visualized by Western blot. GFP recombinant protein was used as negative control. (C) GFP-DDB2–PARP-1 binding assay. U2OS cells transfected with the indicated GFP constructs were lysed in denaturing buffer and subjected to immunoprecipitation with GFP-TRAP beads. The eluate was separated by SDS-PAGE, and GFP-DDB1 or GFP-DDB2 was isolated from polyacrylamide gels (red squares). The proteins were subjected to immunoprecipitation with GFP-TRAP beads and incubated with 100 ng of purified recombinant PARP-1. The beads were processed for immunoblotting. WB, Western blot.

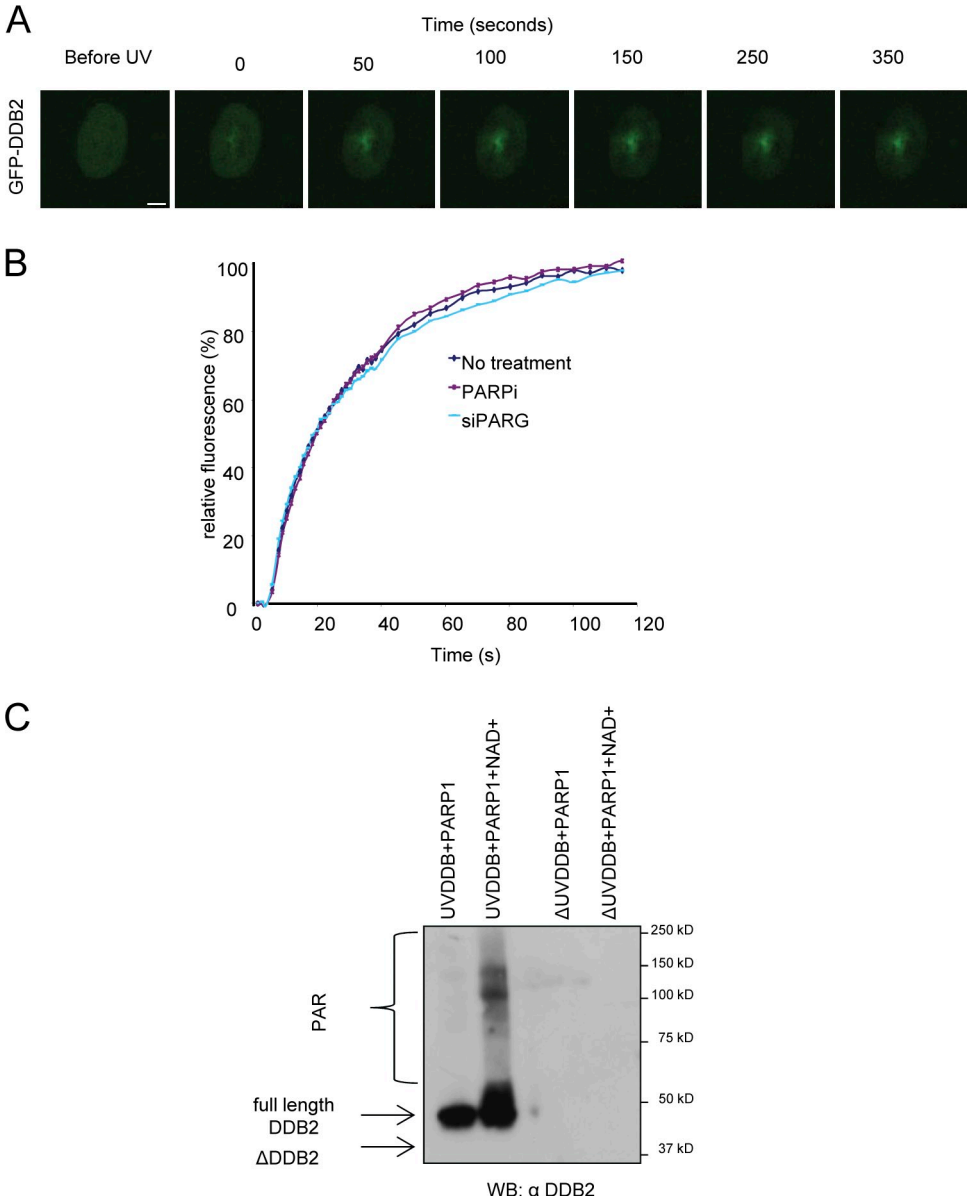


Figure S2. **The kinetics of GFP-DDB2 accumulation is not affected by PARPi or depletion of PARG.** (A) Real-time recruitment of GFP-DDB2 in NHFs at the site of DNA damage using UV-C (266 nm) laser irradiation. Bar, 7.5 µm. (B) NHF cells stably expressing the GFP-DDB2 were transfected with the indicated siRNA or treated with 10 µM PARPi. 48 h after transfection, the cells were UV damaged using UV-C (266 nm) laser irradiation. GFP fluorescence intensities at the site of UV damage were measured by real-time imaging until they reached a maximum. Assembly kinetic curves were derived from at least six cells for each protein. Relative fluorescence was normalized at 0 (before damage) and 100% (maximum level of accumulation). Error bars indicate SEM. (C) In vitro PARylation experiments using purified components. Antibody against the N terminus of DDB2 revealed that DDB2 is directly modified by PARP1. DDB2 lacking its first 40 N-terminal amino acids (ΔUV-DDB) was not detectable. WB, Western blot.

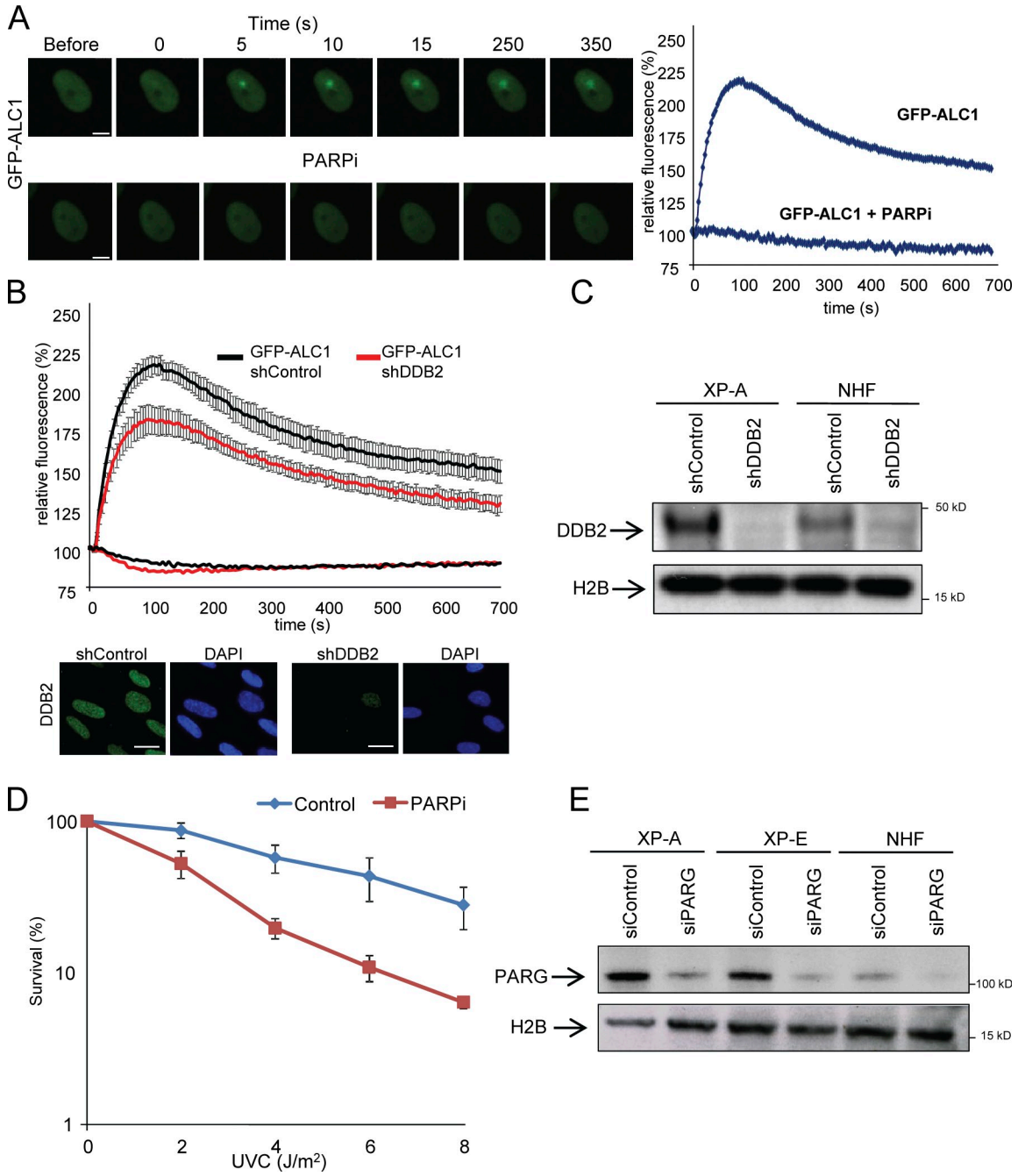


Figure S3. **Transient recruitment of GFP-ALC1 to sites of UV-C laser–induced DNA damage.** (A) Real-time recruitment of GFP-ALC1 in NHFs in the presence or absence of 10 µM PARPi at the site of DNA damage using UV-C (266 nm) laser irradiation. (B) NHF cells stably expressing GFP-ALC1 were infected with the indicated shRNA. The cells were UV damaged using UV-C (266 nm) laser irradiation. GFP fluorescence intensities at the site of UV damage were measured by real-time imaging until they reached a maximum. Assembly kinetic curves were derived from at least six cells for each protein. Error bars indicate SEM. Bars: (A) 7.5 µm; (B) 20 µm. (C) Anti-DDB2 and histone H2B Western blots of total lysates from NHF and XP-A cells expressing shRNAs targeting DDB2 or a nontargeting shControl (mock). (D) Clonal survival of UV-irradiated NHF cells in the presence or absence of 1 µM PARPi. The percentage of surviving cells is plotted against the applied UV-C dose (J/$m^2$). The results are from three independent experiments. Error bars indicate SD. (E) Anti-PARG and histone H2B Western blots of total lysates from XP-A, XP-E, and NHFs transfected with siRNA targeting PARG or a nontargeting siControl (mock).

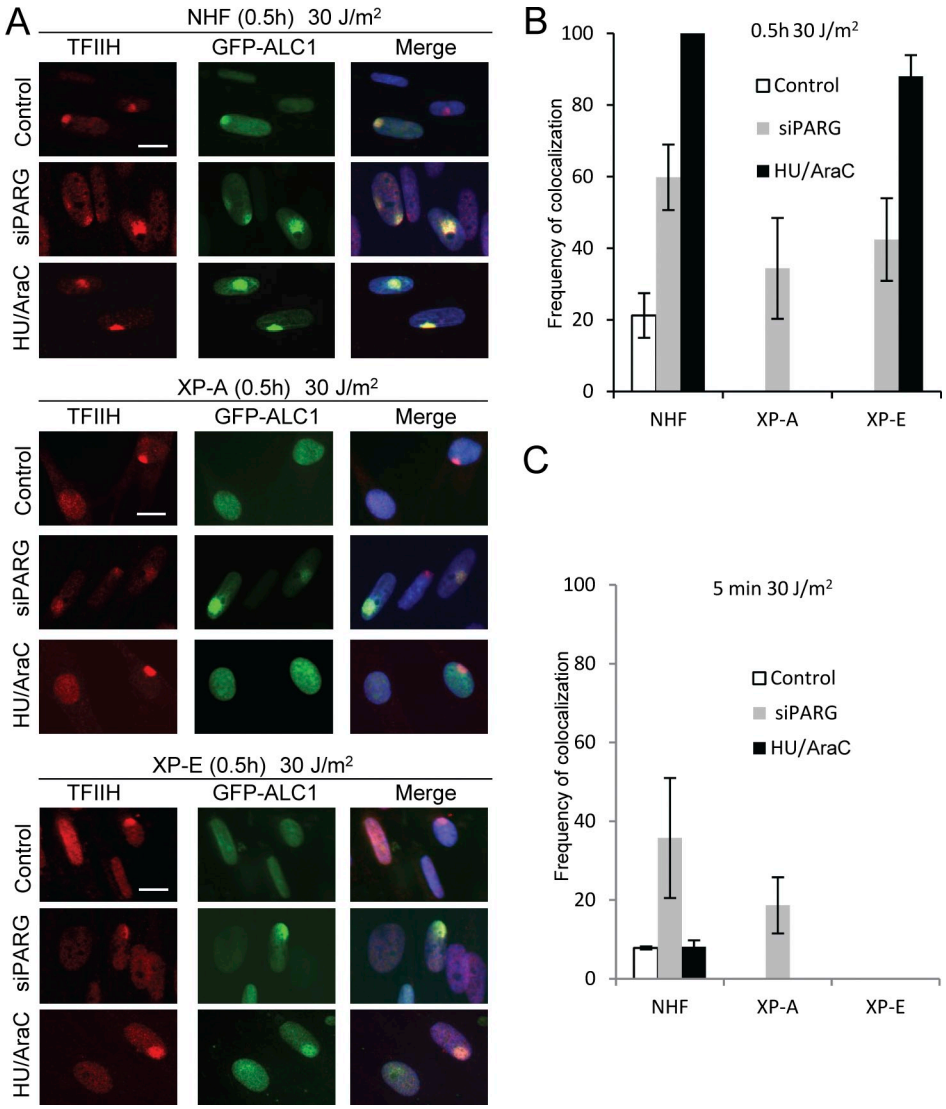


Figure S4. **ssDNA gaps trigger robust GFP-ALC1 recruitment after UV irradiation of normal human and XP-E cells.** (A) NHF, XP-E, and XP-A cells stably expressing GFP-ALC1 transfected with the indicated siRNA or treated with HU/AraC were locally UV exposed to 30 J/m$^2$, fixed after the indicated time, and stained with an antibody recognizing TFIIH. Bars, 20 µm. (B) The percentage of colocalization of GFP-ALC1 with TFIIH in NHF, XP-A, and XP-E cells after 0.5 h of UV local damage is plotted for the different siRNA transfections and HU/AraC treatment. (C) The percentage of colocalization of GFP-ALC1 with TFIIH in NHF, XP-A, and XP-E cells after 5 min of UV local damage is plotted for the different siRNA transfections and HU/AraC treatment. The data shown are from a single representative experiment out of three repeats. (B and C) The results are from three independent experiments in which about 100 cells per condition were analyzed. Error bars indicate SD.

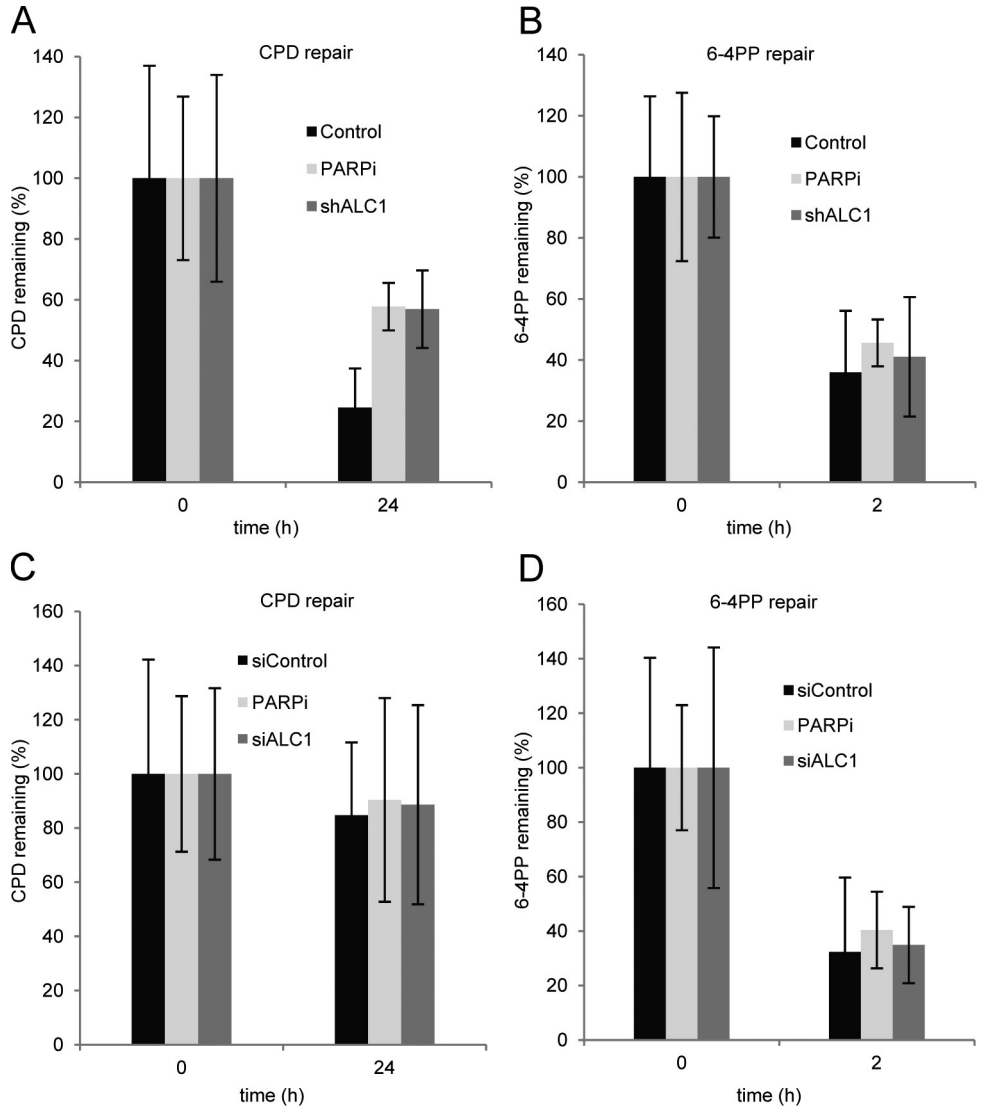


Figure S5. **Significant reduction in CPD repair upon ALC1 depletion or chemical inhibition of PARP1.** (A and B) NHF cells expressing shControl or shALC1 or treated with 10 µM PARPi were irradiated with 10 J/m$^2$ UV-C; CPDs and 6-4PPs were detected immediately and 24 or 2 h, respectively, after UV treatment by ELISA assay. (C and D) XPE cells siRNA transfected or treated with 10 µM PARPi were irradiated with 10 J/m$^2$ UV-C; CPDs and 6-4PPs were detected immediately and 24 or 2 h, respectively, after UV treatment by ELISA assay. The results are from three independent experiments. (A–D) Error bars indicate SD.

Table S1. **Proteins identified in Flag immunoprecipitated material from FLAG-DDB2 expressing MRC5 cells mock treated or irradiated with 20 J/m$^2$ UV-C**

| −UV | | | +UV | | |
|---|---|---|---|---|---|
| **Protein** | **Protein score** | **Unique peptides** | **Protein** | **Protein score** | **Unique peptides** |
| DDB2 | 274 | 9 | DDB2 | 305 | 13 |
| DDB1 | 462 | 24 | DDB1 | 263 | 16 |
| PARP1 | 172 | 6 | CUL4B | 221 | 9 |
| CUL4B | 65 | 4 | PARP1 | 126 | 6 |
| GPS1 | 65 | 1 | COPS4 | 103 | 3 |
| CUL4A | 44 | 1 | CUL4A | 83 | 1 |
| | | | GPS1 | 65 | 1 |
| | | | COPS7A | 64 | 1 |

A unique peptide is defined as a peptide, irrespective of its length, that exists only in one protein of a proteome of interest.